Free Antineutrino Absorption Cross Section. II. Expected Cross Section from Measurements of Fission Fragment Electron Spectrum*

R. E. CARTER, F. REINES, J. J. WAGNER, AND M. E. WYMAN†
Los Alamos Scientific Laboratory, University of California, Los Alamos, New Mexico
(Received September 8, 1958)

A measurement of the electron spectrum from the thermal neutron fission of U^{235} is described. From this spectrum the antineutrino spectrum is calculated, and on the basis of the two-component theory of the antineutrino a predicted average cross section for the absorption of antineutrinos by protons is $(6.1\pm1)\times10^{-43}$ cm²/fission. This agrees with the measured cross section of $(6.7\pm1.5)\times10^{-43}$ cm²/fission. The four-component theory of the antineutrino would have predicted $(3.05\pm0.5)\times10^{-43}$ cm²/fission.

I. INTRODUCTION

IN the preceding paper[1] a measurement of the cross section for the reaction $p(\bar{\nu},\beta^+)n$ for antineutrinos from fission fragments is described. In order to predict the average cross section for this reaction, one needs to know the energy spectrum. A measurement of the electron (beta) energy spectrum from fission permits a determination of the end-point distribution for beta emitters involved. Since this is also the end-point distribution for the antineutrino spectra, one can calculate the required antineutrino spectrum. Muehlhause and Oleksa[2] made such a measurement but their results did not permit an unambiguous interpretation of the cross section in terms of the two-component or four-component theory of the antineutrino.

In the present experiment (Fig. 1) a single plastic scintillator was used as the electron spectrometer. This type of detector has a low gamma sensitivity with nearly 100% efficiency for electron detection. A gas-flow proportional counter placed between the fission source and the scintillator was used as a transmission counter to signal the passage of an electron through it into the scintillator. With this system for gating a pulse-height analyzer, the number of events subjected to pulse-height analysis was about $\frac{1}{4}$ the total scintillator counts. The source of fission-fragment electrons was made the collecting electrode of a fission counter. This scintillation spectrometer with its known source geometry and a suitable energy calibration was used to measure the number of electrons per fission as a function of energy from 1.5 to 8 Mev.

II. EXPERIMENTAL TECHNIQUES

The electron detector (Fig. 1) was a right circular cylinder of Plastifluor B,[3] $1\frac{1}{2}$ inches long and $1\frac{1}{2}$ inches in diameter, cemented to a Dumont-6292 photomultiplier. A foil of U^{235} was placed in an external thermal neutron beam of the Omega West Reactor (OWR). This beta source was located on the axis of the scintillator cylinder and was sufficiently distant so that all detected electrons traveled in essentially parallel paths. The maximum path in the scintillator was 4 g/cm², about the maximum range of an 8-Mev electron. The resolution (full width at half-maximum) for monoenergetic electrons was 18.5% for the 624-kev Cs^{137} line, and 15.3% for the 976-kev Bi^{207} line (K-conversion lines only).

The 1.0639-Mev gamma ray of Bi^{207} which converts in both the K and L shells to give an effective electron line of 0.991 Mev (for the resolution of this system) was adopted as a convenient calibration standard (Fig. 2). An aluminum absorption measurement, using other conversion lines of Bi^{207} ($E_\gamma=0.570$ Mev) and Cs^{137} ($E_\gamma=0.660$ Mev) indicated an energy loss of 0.043 Mev at the 0.991-Mev line due to the materials present between the source and the detector. A measurement of the Tl^{208} (ThC″) electron line at 2.526 Mev proved that the energy scale was linear within 1%. The measured end points of the beta spectra of F^{20} and Al^{28} agreed with the well-known values of 5.41 and 2.87 Mev, respectively (maximum uncertainty 2%). In the course of the present experiment the Rh^{104} end point was found to be 2.45 Mev.

The proportional counter of Fig. 1 was made of two parallel subcounters with a square cross section and 0.005-inch steel center wires. The common wall between these two subcounters and the two windows through which the electrons passed were 0.00025-inch aluminized Mylar. This system was chosen because it gave a relatively small spread in pulse heights from mono-

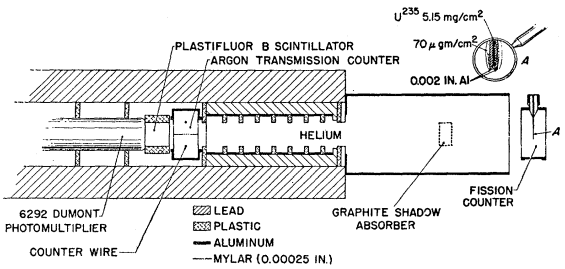

FIG. 1. The experimental arrangement.

* Work performed under the auspices of the U. S. Atomic Energy Commission.
† Present address: University of Illinois, Champaign, Illinois.
[1] F. Reines and C. L. Cowan, Jr., Phys. Rev. **113**, 273 (1959), preceding paper.
[2] C. O. Muehlhause and S. Oleksa, Phys. Rev. **105**, 1332 (1957); and private communication.
[3] Pilot Chemicals, Inc., 47 Felton Street, Waltham 54, Massachusetts.

energetic electrons of minimum specific ionization (less than 50% full width at half-maximum). It also gave variations in the time of formation of the pulse after the electron had traversed the counter of less than 0.5 μsec. The counter gas, 97% argon and 3% ethane, flowed continuously. The height of the most probable pulse produced in the transmission counter by 991-kev electrons corresponded to an energy loss of 4.2 kev, so that the total energy lost by such an electron in traversing the counter (including the Mylar windows) was about 5.5 kev.

The pulses from the photomultiplier were amplified by both a relatively slow (0.3 μsec rise time) linear amplifier, and a fast (0.1 μsec rise time) amplifier (Fig. 3). The signal from the fast amplifier together with that from the transmission counter, was fed to a coincidence circuit, whose output gated a 100-channel analyzer in which the signal from the slow amplifier was analyzed. The widths of the pulses in the coincidence circuit (1 μsec total) and the width of the gating signal to the analyzer (4 μsec) were narrow enough so that, with the geometry and the counting rates employed, not more than 0.1% of the analyzed counts could have been due to accidental β–β or β–γ coincidences.

Studies made with a pulser on the pulse widths and delays of the two channels of the coincidence circuit proved that the coincidence and gating system was 100% efficient. An additional empirical check on the entire electronic system was made by comparing the singles counting rate in the scintillator with the number of analyzed counts for a pure beta-emitting source. This measurement gave an efficiency greater than 95%.

The purpose of the lead shield shown in Fig. 1 was to reduce the background caused by the reactor. The number of electrons from the source which might be scattered into the scintillator by the lead was reduced by the polyethylene ring system. The scintillator itself defined the solid angle for detection. In order to minimize the energy loss of the electron before it entered

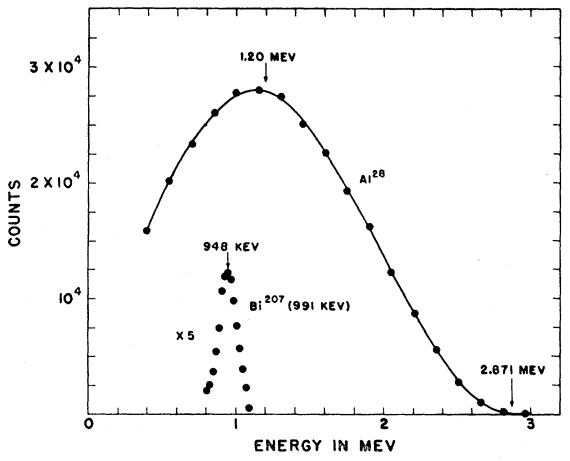

FIG. 2. Al^{28} beta spectrum and Bi^{207} calibration.

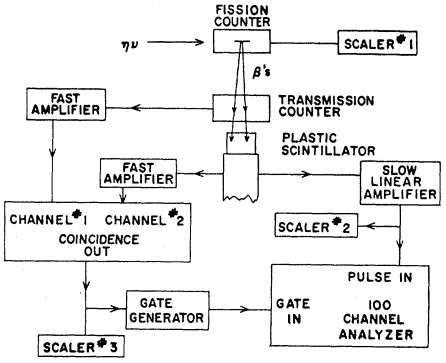

FIG. 3. Block diagram of electronic circuits.

the scintillator, the lead collimator and its 5-inch-diameter aluminum extension were capped with 0.00025-inch Mylar, and the chamber thus formed was filled with helium.

For a point source, the background could be obtained by absorbing the electrons in a conical shadow shield placed at the appropriate point between the source and detector. Such a shadow cone would remove only the primary electrons and would allow a proper subtraction from the gross counting rate. A finite source did not permit this, and a shadow cone placed at even the optimum position removed some of the electrons which should properly be considered background. For the present measurements, a $\frac{3}{4}$-inch-thick graphite shadow shield was inserted as shown in Fig. 1, and the resulting counts were subtracted as background. This left a net count which tended to be too large. On the other hand, without the shadow shield, some electrons which started from the source towards the scintillator were scattered out by gas and windows before reaching it. This gave too low a counting rate. Indications were (from an independently calibrated Bi^{207} source) that neither of these two effects, which tended to compensate, was greater than 10%.

In order to compute the number of betas per fission from the geometry of the system, it was necessary to know the number of fissions, and the point from which the betas were emitted. This was accomplished by sandwiching about 5 mg/cm^2 of U^{235} between two $\frac{3}{4}$-inch disks of 0.002-inch-thick aluminum and coating the outside of one of these disks with $\sim$70 μg/cm^2 of U^{235}. This sandwich was made the collecting electrode of a fission counter, and was located in a neutron beam of 10^6 neutrons per cm^2 per sec. The aluminum foils were thick enough to prevent all fission fragments produced in the center from escaping (and thereby located the beta source) but thin enough so that they did not attenuate the neutron beam nor absorb much energy from the betas emitted towards the scintillator. By counting the number of fissions produced in the monitor coating of uranium and knowing the relative weights of the two deposits, the total fission source strength was obtained to an accuracy of about 2%.

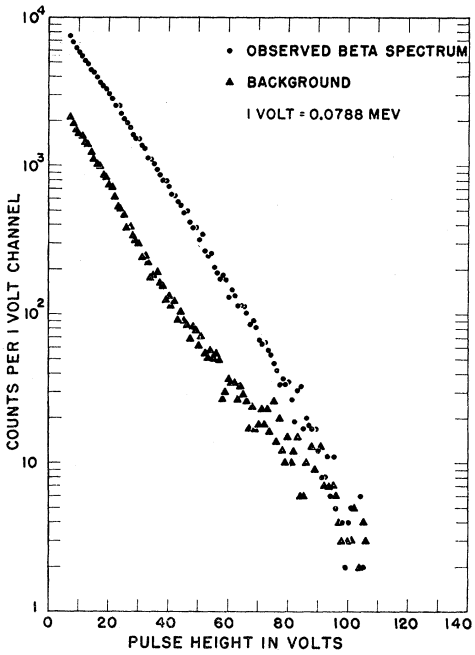

FIG. 4. Fission beta data as taken from the 100-channel analyzer.

The operating schedule of the reactor did not permit foil irradiations long enough to reach effective secular equilibrium. In fact, the data of Fig. 4 were taken $1\frac{1}{2}$ to $2\frac{1}{2}$ hr. after the start of irradiation. However, the calculations of Nelms and Cooper,[4] which give the U^{235} fission product decay spectrum as a function of time, were used to estimate the subsequent behavior. While the expected increase at 1.7 Mev was 6% it declined to 3% at 2 Mev and was less than 1% at 4 Mev and above. The only experimental verification of the procedure used in making the estimate was a series of spectra taken after from 1 to 7 hours of irradiation. The observed changes were consistent with the computed behavior.

III. CORRECTIONS

After a 2% counting-rate correction (analyzer dead time=0.6 msec) and background subtraction were made, the spectrum was raised 0.063 Mev to compensate for the energy loss in the materials between the beta-emitting fission fragment and the plastic detector.

If the resolution function of the system (its response to monoenergetic radiation) is known, the correction for a continuous spectrum is straightforward.[5] Since monoenergetic electrons in the region of 1.5 to 8 Mev were not available, the resolution function could not be measured. The probable form of this function must be considered in order to estimate the effect on the final result.

An electron stopped in a scintillator produces a finite number of photons. The statistics of this process give a predictable Gaussian resolution function. However, some of the electrons incident on a scintillator do not deposit all their energy in it. Some electron energy is lost to bremsstrahlung, the photons escaping from the scintillator. The total energy going into bremsstrahlung for a plastic of this type is less than 3% in the important energy region of the spectrum (between 2.5 and 5 Mev).

Some of the electrons entering the scintillator are scattered back out the front surface without depositing their full energy. The backscattering from this scintillator material has been observed to be 4% for the beta spectrum of Yt^{90}, which has an end-point energy of 2.18 Mev.[6] The fraction of electrons back-scattered at higher electron energies is assumed not to increase markedly. The effect of electrons which scatter out the sides of the scintillator was studied for the fission beta spectrum. For the data taken with the $1\frac{1}{2}$-inch scintillator, the scintillator itself determined the aperture of the system and should exhibit a maximum edge effect. With a larger scintillator ($2\frac{1}{2}$ inches in diameter by 3 inches thick) the shield acted as a somewhat inefficient collimator with at least half the scintillator area shielded. The spectral shapes as seen by the two dissimilar systems were identical but the larger scintillator gave about 5% more betas per fission at all energies. This set an upper limit on the number of electrons scattered out the sides of the $1\frac{1}{2}$-inch scintillator, since the uncertainty in the geometry for the larger system could account for the entire difference. This also demonstrated that the small scintillator was thick enough to analyze the high-energy end of the spectrum.

Hence, the resolution function is the sum of two components. The first is the Gaussian resulting from about 90% of the electrons which deposit their full energy in the scintillator. Its effect on the true spectrum, a relatively small displacement upward in energy, has been computed to be 3 kev at 1 Mev, increasing to 48 kev at 8 Mev.

The form of the other component, corresponding to the reamining 10% of the electrons, is unknown, except that it will appear as a "tail" on the low-energy side of the Gaussian. Various experimentalists[7] have found that the shape of the "tail" may range from exponential to rectangular. A rectangular tail extending to zero energy has the greatest effect on the spectrum. In this case the observed spectrum above 1.5 Mev would be too low by the full 10%. At 1 Mev the correction would be about 7%. Only somewhere below 0.5 Mev would the curve rise above the true value. It should be noted that the Al^{28} spectrum of Fig. 2 requires an equivalent correction of about 5% to obtain agreement with the theoretical shape.

[4] A. T. Nelms and J. W. Cooper, National Bureau of Standards Report NBS-5853 (unpublished).

[5] G. E. Owen and H. Primakoff, Phys. Rev. **74**, 1406 (1948); Rev. Sci. Instr. **21**, 447 (1950), Part II.

[6] D. C. Müller, Anal. Chem. **29**, 975 (1957).

[7] H. W. Koch and J. M. Wyckoff, J. Research Natl. Bur. Standards **56**, 319 (1956); Freedman, Novey, Porter, and Wagner, Rev. Sci. Instr. **27**, 716 (1956).

IV. RESULTS

The distribution of scintillator pulse heights for the electrons emitted from fission fragments is shown in Fig. 4. The background obtained with a $\frac{3}{4}$-inch thickness of graphite as a shadow absorber is shown on the same figure. During the course of experimentation the fission beta spectrum was measured with different solid angles, with and without shielding, and with different detectors. In each case the shape of the spectrum above 1 Mev was the same (within statistics). The data presented here are from the experimental system as described and represent only one of the many measurements. The data corrected as indicated in Sec. III and transformed to betas per fission per Mev are shown in Fig. 5. An analytic function which fits the experimental data in the important energy region is

$$Y(E_\beta)=3.88\exp[-0.575E_\beta-0.055E_\beta^2]. \quad (1)$$

(E_β is the electron kinetic energy in Mev.) It is represented by the solid line on Fig. 5. With this analytic expression, a beta-spectra end-point distribution was calculated on an IBM-704 electronic computing machine for emitters with $Z=32$ and also for $Z=60$ (Fig. 6). From these end-point distributions the antineutrino spectra were calculated. For the details of this calculation see Appendix II. These spectra are shown in Fig. 5, along with the beta spectrum.

The antineutrino absorption cross section per fission is then given by

$$N\bar{\sigma}=\int_{1.8\text{ Mev}}^{\infty}\sigma(E_{\bar{\nu}})\rho(E_{\bar{\nu}})dE_{\bar{\nu}}, \quad (2)$$

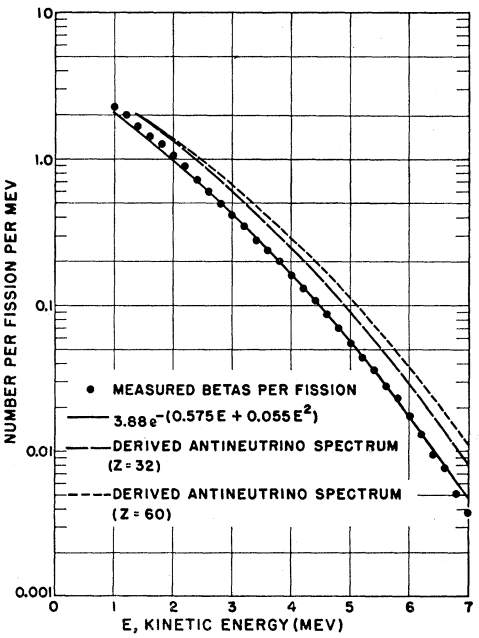

FIG. 5. Corrected results, the empirical fit to the data, and the derived antineutrino spectra.

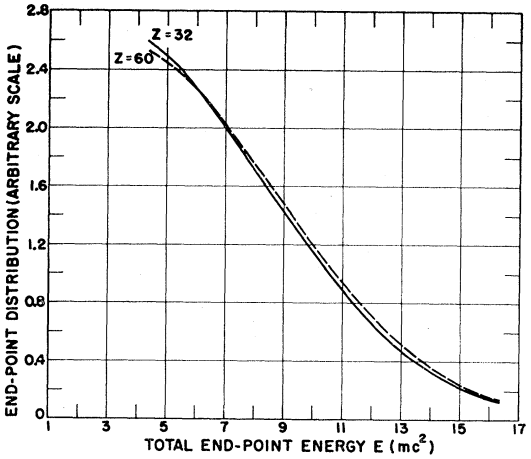

FIG. 6. The end-point distribution, assuming allowed shapes for the individual spectra.

where $\sigma(E_{\bar{\nu}})$ = the theoretically predicted cross section as a function of the antineutrino energy (for details see Appendix I), and $\rho(E_{\bar{\nu}})$ = the number of antineutrinos per fission per Mev at energy $E_{\bar{\nu}}$.

The number of antineutrinos per fission above the threshold for the reaction is

$$N=\int_{1.8\text{ Mev}}^{\infty}\rho(E_{\bar{\nu}})dE_{\bar{\nu}}. \quad (3)$$

The average absorption cross section per antineutrino above the threshold for the reaction is

$$\bar{\sigma}=N\bar{\sigma}/N. \quad (4)$$

From the values of $\rho(E_{\bar{\nu}})$ given in Fig. 5, $N\bar{\sigma}$, N, and $\bar{\sigma}$ were calculated for $Z=32$ and 60. The results are shown in Table I. The average of the two values is listed in line 3. The last line shows the final result adjusted for errors as indicated under reliability.

V. RELIABILITY

It was difficult to determine the errors in an experiment of this type where absolute values of quantities were required. The following is a list of sources of error and an estimate of their effect on the final cross section prediction ($N\bar{\sigma}$).

a. The mass ratio of the uranium source foil to the monitor foil had a uncertainty of $\pm 1\%$ and the fission counter had a plateau sufficiently good so that the uncertainty in the total number of fissions was $\pm 2\%$.

b. The energy calibration proved to have an uncertainty of not greater than $\pm 1\%$.

c. Concern about the effect of the shield system and the method of subtracting background led to a measurement both with and without a shield. Background was measured by replacing the fission foil with an aluminum disk of the size of the foil backing material. The electron spectra in the two cases were identical (within

TABLE I. Summary of results for reaction $p(\bar{\nu},\beta^+)n$.

	$N\bar{\sigma}$ (10^{-43} cm^2/fiss)	N ($\bar{\nu}$/fiss)	$\bar{\sigma}$ (10^{-43} cm$^2/\bar{\nu}$)
$Z=32$	5.21	1.84	2.83
$Z=60$	6.19	2.02	3.06
Average	5.70	1.93	2.95
Adjusted best value	6.1±1	2.1±0.2	2.9±0.44

statistics). The shadow absorber technique used should give an answer which is most nearly correct. The estimate of the uncertainty using this technique was ±5%.

d. The uncertainty in applying the corrections due to the energy shift because of resolution and because of energy loss was ±1%.

e. The analytic fit to the experimental data was estimated to have an uncertainty of ±2%.

f. There is an uncertainty in the theoretical cross section for monoenergetic antineutrinos of ±13% caused by the uncertainty in the measured neutron half-life (12±1.5 min).

g. The precise distribution of Z's of the fission product beta emitters was not known. The use of the average of the values computed for $Z=32$ and $Z=60$ should involve an uncertainty no greater than ±5%.

The arithmetic sum of the above errors is 30%, but it seems reasonable to believe that the correct answer should fall within ±15%.

There is an uncertainty which is not included in the above. Very little experimental data were obtained to determine the asymmetrical part of the resolution function for the scintillator and the departure of the fission beta spectrum from secular equilibrium. Both of these effects tend to give an answer for $N\bar{\sigma}$ which is too low. Since it was estimated that the resolution correction could raise the spectrum by as much as 10% the results should be increased by 5% with an uncertainty of 5%. A further increase of 2±2% should be an adequate allowance for the departure from equilibrium. A 7% correction was made to obtain the values in the last line of Table I.

A calculation of N (the number of antineutrinos per fission above 1.8 Mev) involves all the uncertainties listed above except the one in the theoretical cross section due to the neutron half-life. Hence, the result has been quoted with an uncertainty of ±10%.

The average cross section per antineutrino above 1.8 Mev [Eq. (4)] is determined by a ratio so some of the uncertainties will cancel since they appear in both the numerator and denominator. However, the value will have the uncertainty of the theoretical cross section. An uncertainty of ±15% has been ascribed to this average cross section.

VI. INTERPRETATION OF RESULTS

The measured cross section for the reaction $p(\bar{\nu},\beta^+)n$ for antineutrinos from fission fragments is $N\bar{\sigma}=(6.7\pm1.5)\times10^{-43}$ cm^2/fission.[1] This result is in agreement with theoretical expectation, $N\bar{\sigma}=6.1\pm1\times10^{-43}$ cm^2/fission, based on the measured fission β^- spectrum, the two-component theory of the neutrino, the principle of microscopic reversibility, and the measured characteristics of neutron decay.[8] A more precise measurement of the absorption cross section is of interest in order to sharpen our conclusions and indeed such increased precision is now feasible.[1] In addition to these conclusions based on the measurement of the electron spectrum, we have also calculated in Appendix III the expected cross section for the reaction $Cl^{37}(\nu,\beta^-)A^{37}$. The two-component theory predicts no interaction as does the four-component theory with distinguishable neutrino and antineutrino. A four-component Majorana neutrino theory on the other hand predicts the result 1.44×10^{-44} cm^2/fission. The work of R. Davis is not inconsistent with a zero cross section.

VII. ACKNOWLEDGMENTS

The authors wish to thank Mr. E. H. Kinney for assistance with the numerical computations, members of the Physics Division reactor group for helpful discussions, and Mr. J. G. Povelites and Dr. E. H. VanKooten for the preparation and weighing of the fission foils.

APPENDIX I. PREDICTED CROSS SECTION FOR $p(\nu,\beta^+)n$

For a monoenergetic $\bar{\nu}$ as derived for the four-component neutrino by Konopinski[9] and others,

$$\sigma(E_{\bar{\nu}})=\frac{G^2}{2\pi}\left(\frac{\hbar}{mc}\right)^2\left(E_{\bar{\nu}}-\frac{M_n-M_p}{m}\right)\times\left[\left(E_{\bar{\nu}}-\frac{M_n-M_p}{m}\right)^2-1\right]^{\frac{1}{2}},\quad(5)$$

where M_n-M_p is the neutron-proton mass difference, $E_{\bar{\nu}}$ is the antineutrino energy in mc^2 units, and G^2 is the appropriate β coupling constant. The threshold is at 3.530 electron masses or 1.804 Mev. According to DuMond and Cohen,[10] $(\hbar/mc)^2=1.491\times10^{-21}$ cm^2. As pointed out by Lee and Yang,[11] and others, the formula can be generalized to include the two-component neutrino by the addition of a factor P, which is unity in the

[8] An independent prediction made by King and Perkins from a consideration of the details of the fission chains gives for the two-component neutrino theory the result $N\bar{\sigma}=8.5\times10^{-43}$ cm^2/fission [R. W. King and J. F. Perkins, Phys. Rev. **112**, 963 (1958)]. We wish to thank Dr. King for this information in advance of publication.

[9] E. Konopinski *et al.* (private communication, 1953).

[10] J. W. M. DuMond and E. R. Cohen, Phys. Rev. **82**, 555 (1951).

[11] T. D. Lee and C. N. Yang, Phys. Rev. **105**, 1671 (1957).

four-component theory and two for the two-component theory. This result follows from the restriction in the two-component theory of the final states in the neutron decay.

$$\sigma(E_{\bar{\nu}})=P(G^2/2\pi)\times 1.491\times 10^{-21}(E_{\bar{\nu}}-2.530)\times[(E_{\bar{\nu}}-2.530)^2-1]^{\frac{1}{2}}, \quad (6)$$

where P is the parity factor and $P=1$ for a four-component $\bar{\nu}$, $P=2$ for a two-component $\bar{\nu}$. $G^2/2\pi=\alpha$ is evaluated from the properties of neutron decay. When G^2 is redefined in terms customarily used in β-decay theory, $G^2=g^2\times m^2/\hbar^4$.

$$\frac{1}{\tau_n}=g^2\frac{m^5c^4F(\eta_0)}{2\pi^3h^7},$$

where τ_n (the neutron mean life)$=1040\pm 130$ sec.[12]

The β^- spectrum from neutron decay measured by Robson[13] is consistent with an allowed shape having an end point of 782 kev. Hence the Fermi function $F(\eta_0)=F(P_{\max}/_{mc})=F(2.324)=1.633$.

$$\alpha=\frac{\pi^2}{c}\frac{\hbar^3}{(mc)^3}\frac{1}{\tau_nF(\eta_0)}=(1.12\pm 0.14)\times 10^{-44}\ \text{cm}^2.$$

The desired cross section for a monoenergetic antineutrino is

$$\sigma(E_{\bar{\nu}})=(1.12\pm 0.14)\times 10^{-44}(E_{\bar{\nu}}-2.53)\times[(E_{\bar{\nu}}-2.53)^2-1]^{\frac{1}{2}}\times P\ \text{cm}^2. \quad (7)$$

APPENDIX II. CROSS SECTION FOR FISSION FRAGMENT ANTINEUTRINOS

The β^- spectrum from fission fragments differs from the associated $\bar{\nu}$ spectrum because of the finite mass of the electron and the spectral distortion due to electrostatic attraction between the electron and nucleus. Since, given an end point and Coulomb factor, both the β^- and $\bar{\nu}$ spectrum are determined, the problem is viewed as one of determining the end-point distribution, considering Coulomb effects. However, the details of the short-lived fission product chains are not known and hence it is not possible to predict these effects accurately. Consequently, a procedure was adopted which enabled the expected cross section to be bracketed. It was assumed that the observed β^- spectrum results from the superposition of a continuous distribution of β^- emitters, each one having an allowed shape but all with the same nuclear charge Z. Two extreme values of $Z(Z=60, 32)$ are assumed so as to place upper and lower limits on the Coulomb distortion of the β^-, and hence the $\bar{\nu}$ spectrum. The end-point distribution is then determined by solving the appropriate integral equation, and the cross section of Appendix I is integrated over the resulting $\bar{\nu}$ spectrum.

The experimentally determined β^- spectrum $Y(E_\beta)$ is related to the end-point distribution $n(E,Z)$ by the integral equation

$$Y(E_\beta)=\int_{E=E_\beta}^{\infty} n(E,Z)B(E,Z)f(E,E_\beta,Z)dE, \quad (8)$$

where $B(E,Z)$ is the normalization function for the allowed β^- spectrum $f(E,E_\beta,Z)$,

$$B^{-1}(E,Z)=\int_{E_\beta=1}^{E} f(E,E_\beta,Z)dE_\beta, \quad (9)$$

and E_β is the total beta energy, including the rest energy. In general

$$f(E,E_\beta,Z)=E_\beta^2(E-E_\beta)^2G(Z,P_\beta), \quad (10)$$

where

$$G(Z,P_\beta)=(P_\beta/E_\beta)F(Z,P_\beta). \quad (11)$$

F is the Fermi Coulomb function,[14] and P_β is the electron momentum.

For $Z=32$, $G(32,P_\beta)=a$, which is constant to $\pm 6\%$, and

$$f(32,E_\beta,E)=E_\beta^2(E-E_\beta)^2a. \quad (12)$$

For $Z=60$, $G(60,P_\beta)$ is represented to within $\pm 2\%$ by the function

$$G(E_\beta)=b\exp[-0.16(E_\beta-1)^{\frac{1}{2}}] \quad (13)$$

over the range $1mc^2<E_\beta<15mc^2$. $n(E,Z)$ can now be solved for, assuming Z independent of E. Rewriting (8),

$$M=Y/E^2G=\int_{E=E_\beta}^{\infty} m(E,Z)(E-E_\beta)^2dE, \quad (14)$$

where

$$m(E,Z)=n(E,Z)B(E,Z). \quad (15)$$

Differentiating (14) with respect to E_β three times,

$$m(E_\beta,Z)=\tfrac{1}{2}d^3M(E_\beta)/dE_\beta^3, \quad (16)$$

and the end-point distribution is obtained from (15) and (16).

The fission fragment $\bar{\nu}$ spectrum $\rho(E_{\bar{\nu}},Z)$ is then given by adding the spectra having the calculated end-point distribution $n(E,Z)$:

$$\rho(E_{\bar{\nu}},Z)=\int_{E=E_{\bar{\nu}}+1}^{\infty} n(E,Z)B(E,Z)f'(E_{\bar{\nu}},E,Z)dE. \quad (17)$$

For $Z=32$, $f'=(E-E_{\bar{\nu}})^2E_{\bar{\nu}}^2$,

$Z=60$, $f'=(E-E_{\bar{\nu}})^2E_{\bar{\nu}}^2\exp[-0.16(E-E_{\bar{\nu}}-1)^{\frac{1}{2}}]$. (18)

[12] Spivak, Sosnosky, Prokofiev, and Sokoloff, *Proceedings of the International Conference on the Peaceful Uses of Atomic Energy, Geneva, 1955* (United Nations, New York, 1956), Vol. 2, p. 33.

[13] J. M. Robson, Phys. Rev. **83**, 349 (1951).

[14] These functions are given by M. E. Rose in *Beta- and Gamma-Ray Spectroscopy*, edited by K. Siegbahn (Interscience Publishers, Inc., New York, 1955), Chap. 9, Appendix.

The average cross section per fission $N\bar{\sigma}$, for the fission $\bar{\nu}$ spectrum, is then given by

$$N\bar{\sigma}(Z)=\int_{E_{\bar{\nu}}=3.53}^{\infty}\sigma(E_{\bar{\nu}})\rho(E_{\bar{\nu}},Z)dE_{\bar{\nu}}. \quad (19)$$

The number N of antineutrinos above a certain energy is

$$N=\int_{E_{\bar{\nu}}}^{\infty}\rho(E_{\bar{\nu}},Z)dE_{\bar{\nu}}. \quad (20)$$

APPENDIX III. EVALUATION OF CROSS SECTION FOR FISSION FRAGMENT NEUTRINO $Cl^{37}(\nu,\beta^-)A^{37}$

In view of the experiment of Raymond Davis searching for this reaction at the Savannah River Plant it seems worthwhile to evaluate the expected cross section. The cross section for a neutrino (or antineutrino) of energy E is given by the expression[15]

$$\sigma_\nu(E)=4\pi^3A\frac{(z+1)}{\tau}\left(\frac{\hbar}{mc}\right)^3\frac{R(z+1,E-E_0)}{4\pi Z^3}\times\frac{1}{\alpha^2C}$$

$$\times\left(\frac{E-E_0}{E_0+1}\right)^2\left\{1-\exp\left[\frac{-2\pi(z+1)\alpha(E-E_0}{[(E-E_0)^2-1]^{\frac{1}{2}}}\right]\right\}^{-1}, \quad (21)$$

where $E_0=0.608mc^2$, $\tau=4.24\times10^6$ sec (mean life), $\alpha=1/137$, and $Z=18$.

[15] R. Davis (private communication). This expression with $A=1$ was derived by Edward Kelley.

TABLE II. Table of A.

Source	Two-component theory	Four-component theory, $\bar{\nu}\equiv\nu$	Four-component theory, $\bar{\nu}\neq\nu$
neutrinos (β^+ decay)	2	1	1
antineutrinos (β^- decay)	0	1	0

TABLE III. Summary of results for reaction Cl^{37} $(\nu,\beta^-)A^{37}$.

	$N\bar{\sigma}\times10^{44}$, cm²/fiss	$\frac{N}{\nu}$/fiss (above 1.61 mc^2)	$\bar{\sigma}\times10^{45}$, cm²/$\nu$
$Z=32$	1.33	4.0	3.4
$Z=60$	1.54	4.2	3.7
Average	1.44	4.1	3.55

$R(z+1, E-E_0)$ is the function defined by Feenberg and Trigg.[16]

The value of A is determined by the source and neutrino theory employed as given in Table II.

The cross section for the only nonzero case, i.e. for the four-component Majorana theory, involving fission product antineutrinos is obtained by integrating the cross section given by Eq. (21) over the antineutrino spectrum. Table III gives these results.

Thus far the Davis experiment gives a result which is not clearly inconsistent with background. It is understood that further work is in progress to increase the sensitivity of the method.[17]

[16] E. Feenberg and G. L. Trigg, Revs. Modern Phys. **22**, 399 (1950).

[17] R. Davis (private communication).